NeuroImage 256 (2022) 119228

Contents lists available at ScienceDirect

NeuroImage

journal homepage: www.elsevier.com/locate/neuroimage

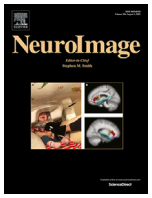

Predicting brain age from functional connectivity in symptomatic and preclinical Alzheimer disease

Peter R. Millar[a,*], Patrick H. Luckett[a], Brian A. Gordon[b], Tammie L.S. Benzinger[b], Suzanne E. Schindler[a], Anne M. Fagan[a], Carlos Cruchaga[c], Randall J. Bateman[a], Ricardo Allegri[d], Mathias Jucker[e,f], Jae-Hong Lee[g], Hiroshi Mori[h], Stephen P Salloway[i], Igor Yakushev[j], John C. Morris[a], Beau M. Ances[a,b], for the Dominantly Inherited Alzheimer Network[**]

[a] Department of Neurology, Washington University, St. Louis, MO 63110, USA
[b] Department of Radiology, Washington University in St. Louis, St. Louis, MO, USA
[c] Department of Psychiatry, Washington University in St. Louis, St. Louis, MO, USA
[d] Department of Cognitive Neurology, Institute for Neurological Research Fleni, Buenos Aires, Argentina
[e] German Center for Neurodegenerative Diseases (DZNE), Tübingen, Germany
[f] Hertie Institute for Clinical Brain Research, University of Tübingen, Tübingen, Germany
[g] Department of Neurology, Asan Medical Center, University of Ulsan College of Medicine, Seoul, South Korea
[h] Department of Clinical Neuroscience, Osaka City University Medical School, Nagaoka Sutoku University, Abenoku, Osaka 545-8585, Japan
[i] Department of Neurology, Brown University, Providence, RI, USA
[j] Department of Nuclear Medicine, Technical University of Munich, Munich, Germany

ARTICLE INFO

Keywords:
Brain aging
Alzheimer disease
Resting-state functional connectivity
fMRI
Machine learning

ABSTRACT

"Brain-predicted age" quantifies apparent brain age compared to normative neuroimaging trajectories. Advanced brain-predicted age has been well established in symptomatic Alzheimer disease (AD), but is underexplored in preclinical AD. Prior brain-predicted age studies have typically used structural MRI, but resting-state functional connectivity (FC) remains underexplored. Our model predicted age from FC in 391 cognitively normal, amyloid-negative controls (ages 18–89). We applied the trained model to 145 amyloid-negative, 151 preclinical AD, and 156 symptomatic AD participants to test group differences. The model accurately predicted age in the training set. FC-predicted brain age gaps (FC-BAG) were significantly older in symptomatic AD and significantly younger in preclinical AD compared to controls. There was minimal correspondence between networks predictive of age and AD. Elevated FC-BAG may reflect network disruption during symptomatic AD. Reduced FC-BAG in preclinical AD was opposite to the expected direction, and may reflect a biphasic response to preclinical AD pathology or may be driven by inconsistency between age-related vs. AD-related networks. Overall, FC-predicted brain age may be a sensitive AD biomarker.

1. Introduction

Magnetic resonance imaging (MRI) has revealed structural and functional brain changes in the progression of Alzheimer disease (AD) (Frisoni et al., 2010; Dennis and Thompson, 2014). Specifically, regional cortical thinning and volume loss are thought to result from neurodegenerative processes and typically occur after amyloid deposition and hyperphosphorylated tau aggregation (Bateman et al., 2012; Jack et al., 2013, 2016). Additionally, differences in resting-state functional connectivity (FC) are thought to reflect disruption of brain networks, particularly in regions with amyloid deposition (Greicius et al., 2004; Hedden et al., 2009; Brier et al., 2012, 2014a).

Recent advances in machine learning have yielded complex, nonlinear, multivariate, predictive models of neuroimaging data. One approach models normative trajectories of neuroimaging features across the adult lifespan to quantify how "old" an individual's brain appears in relation to the normative trajectory. Thus, this "brain-predicted age" framework summarizes complex neuroimaging age relationships into a simple, easily interpretable summary measure (Cole and Franke, 2017; Franke and Gaser, 2019). Deviations from normative trajectories cap-

* Corresponding author.
E-mail address: pmillar@wustl.edu (P.R. Millar).
** Dominantly Inherited Alzheimer Network consortium.

https://doi.org/10.1016/j.neuroimage.2022.119228.
Received 25 January 2022; Received in revised form 28 March 2022; Accepted 19 April 2022
Available online 20 April 2022.

tured by brain-predicted age may yield substantial clinical utility as reliable, personalized biomarkers of physiological processes that underly brain aging and contribute to cognitive decline or reserve.

Several studies have observed advanced brain aging in mild cognitive impairment (MCI) and symptomatic AD (Franke et al., 2010; Franke and Gaser, 2012). Further, brain-predicted age predicts progression from MCI to AD with greater discrimination than simpler structural estimates of hippocampal volume, established cognitive screening tests, or biomarkers of amyloid and tau pathophysiology (Gaser et al., 2013). Beyond AD, brain-predicted age estimates are broadly sensitive to a range of psychiatric and neurological disorders (Franke and Gaser, 2019). Thus, brain-predicted age may provide a comprehensive view of healthy and pathological brain aging above and beyond simpler univariate measures derived from the same imaging data. Hence, brain-predicted age might be useful as a screening or staging tool in early AD. However, it is unknown at what stage of AD progression advanced brain aging first appears. For instance, brain-predicted age may be sensitive to subtle differences associated with preclinical amyloidosis and/or tau pathophysiology. Although previous studies have demonstrated that brain-predicted age is associated with genetic risk of AD (Löwe et al., 2016), as well as with amyloid deposition in Down syndrome (Cole et al., 2017), brain-predicted age has been relatively underexplored in the preclinical stage of late onset AD (i.e., accumulation of amyloid and tau) (Ly et al., 2020).

Moreover, prior brain-predicted age models have focused primarily on structural MRI (Cole and Franke, 2017; Franke and Gaser, 2019). More recent studies have considered additional imaging modalities, including metabolic PET (Goyal et al., 2019) and diffusion MRI (Cherubini et al., 2016). FC-based brain age models have been applied to developmental samples (Dosenbach et al., 2010; Nielsen et al., 2019), but have only recently been applied to older adults and AD cohorts (Eavani et al., 2018; Gonneaud et al., 2021; Liem et al., 2017). Recent multimodal comparisons of FC- and structural MRI-based age prediction have shown that these unimodal estimates are only modestly correlated (Dunås et al., 2021; Eavani et al., 2018) and that multimodal models predict age more accurately than unimodal models (Engemann et al., 2020; Liem et al., 2017). These results are consistent with the interpretation that functional and structural imaging modalities capture complementary age-related signals. Thus, FC might offer a promising avenue for modeling age-related differences and maximizing sensitivity to early AD.

Since FC disruptions have been noted in both healthy age differences and preclinical AD, unrecognized preclinical AD pathology in older adult samples may inflate “healthy aging” effects (Brier et al., 2014b). This influence is particularly relevant in brain-predicted age models, which define normative trajectories based on supplied training data (Ly et al., 2020). The presence of preclinical pathology in training sets will bias the “healthy aging” model and will reduce sensitivity to detect true deviation due to preclinical pathology.

Hence, we aim to develop and validate a model of FC-predicted brain age that controls for preclinical AD pathology. We will test the sensitivity of this model to symptomatic and preclinical AD. We predict that the FC-predicted brain age will be elevated in symptomatic AD, consistent with structural MRI models. Importantly, we test the novel hypothesis that FC-predicted brain age should also be sensitive to subtle network disruptions in preclinical AD. Finally, we evaluate model-specific FC feature importance to compare patterns of network disruption in healthy vs. pathological brain aging.

2. Materials and methods

2.1. Participants

To model differences in functional connectivity across the adult lifespan we combined FC data from three sources: participants enroled in studies at the Knight Alzheimer Disease Research Center (ADRC) at Washington University in St. Louis (WUSTL) (Brier et al., 2012; Millar et al., 2020), healthy controls from existing studies collected by the Ances lab at WUSTL (Ortega et al., 2015; Thomas et al., 2013), and mutation-negative controls in the Dominantly Inherited Alzheimer Network (DIAN) study of autosomal dominant AD at multiple international sites including WUSTL (Chhatwal et al., 2013; McKay et al., 2022; Smith et al., 2021). To train and test the model’s ability to predict age in healthy controls, we limited participants only to those who were cognitively normal, as assessed by the Clinical Dementia Rating (CDR 0) (Morris, 1993), and had at least one biomarker indicating the absence of amyloid pathology (see below). We excluded 59 participants over age 50 who did not have an available CDR or biomarker measures in order to minimize the likelihood of undetected AD pathology in our training set. This set of healthy control participants was randomly split into a training set (~80% of the sample; $N = 391$), in which the model learned to predict age from FC features, and a held-out testing set (~20%; $N = 98$), in which the generalizability of the model was evaluated in unseen data.

Finally, independent samples for residual analyses included three participant groups from the Knight ADRC cohorts: a randomly selected subset of amyloid-negative controls (who were not included in the training or testing sets), amyloid-positive preclinical AD participants, and symptomatic AD participants. Importantly, since we hypothesized that model predictions of brain age should have increased error in the preclinical and symptomatic AD samples, these samples were used only for hypothesis testing and not for evaluating model performance. Moreover, these samples came from a restricted age range, which is not representative of the full adult lifespan sample on which the model was trained. See Table 1 for demographic details of each sample. All procedures were approved by the Human Research Protection Office at WUSTL.

2.2. Assessment of dementia

Cognitive status was assessed annually using the CDR (Morris, 1993). A CDR score of 0 defines cognitive normality, while CDR 0.5, 1, and 2 define very mild, mild, and moderate dementia, respectively. By design, all participants included in the training set, amyloid-negative control, or preclinical AD groups had CDR scores of 0. The symptomatic AD group included participants with CDR > 0 with a biomarker measure consistent with amyloid pathology (see below) and/or a primary diagnosis of AD dementia (McKhann et al., 2011).

2.3. PET & CSF biomarkers

Amyloid burden was imaged with positron emission tomography (PET) using [11C]-Pittsburgh Compound B (PIB) (Mintun et al., 2006) or [18F]-Florbetapir (AV45) (Clark et al., 2011). Regional standard uptake ratios (SUVRs) were modeled from 30 to 60 min after injection for PIB and from 50 to 70 min for AV45, using cerebellar grey as the reference region. Regions of interest were segmented automatically using Freesurfer 5.3 (Fischl, 2012). Global amyloid burden was defined as the mean of partial-volume-corrected SUVRs from bilateral precuneus, superior and rostral middle frontal, lateral and medial orbitofrontal, and superior and middle temporal regions (Su et al., 2013).

Cerebrospinal fluid (CSF) was collected via lumbar puncture using methods described previously (Fagan et al., 2006). After overnight fasting, 20- to 30 mL samples of CSF were collected, centrifuged, then aliquoted (500 µL) in polypropylene tubes, and stored at -80 °C. CSF amyloid β peptide 42 (Aβ42), Aβ40, and phosphorylated tau-181 (pTau) were measured with automated Lumipulse immunoassays (Fujirebio, Malvern, PA) using a single lot of assays for each analyte.

Amyloid positivity was defined using previously published cutoffs for PIB (SUVR > 1.42) (Vlassenko et al., 2016) or AV45 (SUVR > 1.19) (Su et al., 2019). Additionally, the CSF Aβ42/Aβ40 ratio has been shown to be highly concordant with amyloid PET (positivity cutoff < 0.0673) (Schindler et al., 2018; Volluz et al., 2021). Thus, participants were defined as amyloid-positive (for preclinical or symptomatic AD groups) if

Table 1
Demographic information of the combined samples. DIAN = Dominantly Inherited Alzheimer Network, ADRC = Alzheimer Disease Research Center, AD = Alzheimer disease, CDR = Clinical Dementia Rating, MMSE = Mini Mental State Examination, FD = framewise displacement, WUSTL = Washington University in St. Louis, T = Tesla, TR = repetition time. Group differences from the amyloid-negative controls were tested with t tests for continuous variables and $\chi 2$ tests for categorical variables. *** $p < .001$, ** $p < .01$, * $p < .05$, $^{\wedge}$ $p < .10$.

	TRAINING SETS (total $N = 391$)			TEST SETS (total $N = 98$)			ANALYSIS SETS (total $N = 483$)		
Measure	Ances Controls	DIAN Mutation -	Knight ADRC	Ances Controls	DIAN Mutation -	Knight ADRC	Amyloid - Controls	Preclinical AD	Symptomatic AD
N	137	120	134	38	26	34	145	151	156
Age (mean, SD)	30.01 (9.95)	40.02 (10.26)	64.97 (10.57)	26.68 (7.11)	41.46 (12.34)	63.97 (11.31)	66.88 (8.53)	72.69 (6.94)***	75.65 (6.85)***
CDR (N 0 / N 0.5 / N 1 / N 2)	NA	120 / 0 / 0 / 0	134 / 0 / 0 / 0	NA	26 / 0 / 0 / 0	34 / 0 / 0 / 0	145 / 0 / 0 / 0	151 / 0 / 0 / 0	0 / 119 / 35 / 2
Amyloid status (N - / +)	NA	120 / 0	134 / 0	NA	26 / 0	34 / 0	145 / 0	0 / 151	0 / 156
Biomarkers available (N PET / CSF / both)	NA	30 / 6 / 79	11 / 22 / 91	NA	3 / 1 / 21	5 / 0 / 28	24 / 0 / 121	17 / 0 / 134	14 / 0 / 43
APOE ε4 carrier status (N - / +)	NA	85 / 35	99 / 34	NA	19 / 7	28 / 5	115 / 30	68 / 83***	56 / 99***
MMSE (mean, SD)	NA	NA	29.26 (1.05)	NA	NA	29.45 (0.94)	29.12 (1.17)	28.98 (1.33)	25.38 (3.53)***
Sex (N female / male)	70 / 64	76 / 44	84 / 50	19 / 18	16 / 10	22 / 12	90 / 55	92 / 59	68 / 88**
Years of education (mean, SD)	13.68 (2.16)	14.78 (3.04)	16.16 (2.43)	13.95 (1.99)	14.92 (2.83)	16.48 (2.43)	15.68 (2.66)	15.95 (2.64)	15.03 (2.96)*
Race (% white)	44.5%	98.3%	83.6%	45.9%	100%	78.8%	87.6%	88.7%	87.2%
Mean mm FD (mean, SD)	0.11 (0.05)	0.11 (0.05)	0.17 (0.06)	0.11 (0.05)	0.11 (0.04)	0.17 (0.06)	0.18 (0.06)	0.18 (0.06)	0.19 (0.06)
Frames retained (mean, SD)	85% (9%)	82% (11%)	80% (11%)	84% (10%)	85% (10%)	78% (12%)	78% (12%)	78% (11%)	76% (12%)
Site	WUSTL	Multiple sites	WUSTL	WUSTL	Multiple sites	WUSTL	WUSTL	WUSTL	WUSTL
Scanner	Siemens Trio	Siemens Trio / Verio	Siemens Trio / Biograph	Siemens Trio	Siemens Trio / Verio	Siemens Trio / Biograph	Siemens Trio / Biograph	Siemens Trio / Biograph	Siemens Trio / Biograph
Field strength	3T	3T	3T	3T	3T	3T	3T	3T	3T
Voxel size (mm^3)	4.0	3.0 – 4.0	4.0	4.0	3.0 – 4.0	4.0	4.0	4.0	4.0
TR (ms)	2200	2200 – 3000	2200	2200	2200 – 3000	2200	2200	2200	2200
# runs / # frames per run	2 / 164	1 / 120	2 / 164	2 / 164	1 / 120	2 / 164	2 / 164	2 / 164	2 / 164

they had either a PIB, AV45, or CSF Aβ42/Aβ40 ratio measure in the positive range. Since no published thresholds were available for CSF tau positivity, we defined an exploratory threshold by a median split of pTau within the preclinical AD sample (positivity cutoff > 53.15 pg/mL).

2.4. APOE genotype

APOE genotyping was performed using either an Illumina 610 or Omniexpress chip using methods described previously (Cruchaga et al., 2013). We defined $\varepsilon4$ carriers as those with at least one $\varepsilon4$ allele present, that is, $\varepsilon2/\varepsilon4$, $\varepsilon3/\varepsilon4$, and $\varepsilon4/\varepsilon4$, whereas $\varepsilon4$ non-carriers were those without a single $\varepsilon4$ allele present, that is, $\varepsilon2/\varepsilon2$, $\varepsilon2/\varepsilon3$, and $\varepsilon3/\varepsilon3$. The frequencies of *APOE* genotypes per group are presented in Table 1.

2.5. MRI acquisition and preprocessing

All MRI data were obtained using a Siemens 3T scanner, although there was a variety of specific models within and across studies (see Table 1). As described previously, participants in the Knight ADRC (Brier et al., 2012) and Ances lab (Thomas et al., 2013) studies completed identical protocols for structural (sagittal T1-weighted magnetization-prepared rapid gradient echo sequence [MPRAGE] with repetition time [TR] = 2400 ms, echo time [TE] = 16 ms, flip angle = 8°, field of view = 256 mm, 1 mm isotropic voxels; oblique T2-weighted fast spin echo sequence [FSE] with TR = 3200 ms, TE = 455 ms, 256 x 256 acquisition matrix, 1 mm isotropic voxels) and functional imaging (interleaved whole-brain echo planar imaging sequence [EPI] with TR = 2200 ms, TE = 27 ms, flip angle = 90°, field of view = 256 mm, 4 mm isotropic voxels for two 6 min runs [164 volumes each] of eyes open fixation), although there was some variability in the sequence parameters for the DIAN participants (see Table 1) with the most notable difference being shorter resting-state runs (one 5 min run of 120 volumes).

All MRI data were processed using a common pipeline. Multiple resting state runs from a single session were processed together. Initial preprocessing followed conventional methods, as described previously (Brier et al., 2012; Millar et al., 2020; Shulman et al., 2010). Briefly, these steps included frame alignment, debanding, rigid body transformation, bias field correction, and normalization of within-run intensity values to a whole-brain mode of 1000 (Power et al., 2012). Transformation to an in-house atlas template based on 120 independent, cognitively normal older adults (CAPIIO) was performed using a composition of affine transforms connecting the functional volumes with the T2-weighted and MPRAGE images. Frame alignment was included in a single resampling that generated a volumetric timeseries of the concatenated runs in isotropic 3 mm atlas space.

As described previously (Fox et al., 2009; Millar et al., 2020), additional processing was performed to allow for nuisance variable regression. Masks of whole brain, grey matter, white matter, and CSF were generated from T1 images in FreeSurfer 5.3 (Fischl, 2012). Two indices of framewise motion were calculated across the BOLD timeseries, including framewise displacement (FD) and derivative of variance (DVARS). Data were subjected to framewise censoring based on the motion estimates. Specifically, volumes were censored if FD exceeded 0.3 mm or if DVARS exceeded 2.5 SD from the participant's mean. To further minimize the confounding influence of head motion on FC estimates (Power et al., 2012) in all samples, we only included individuals with low estimates of in-scanner head motion (mean FD < 0.30 mm and > 50% frames retained after motion censoring, see Supplementary Fig. S1). BOLD data were subjected to a temporal band-pass filter (0.005 Hz < f < 0.1 Hz) and subjected to nuisance variable regression, including motion parameters, as well as timeseries from the whole brain (global signal), CSF, ventricle, and white matter masks, as well as the derivatives of these signals. Finally, BOLD data were spatially blurred (6 mm full width at half maximum).

2.6. Functional connectivity features

Final BOLD timeseries data were averaged across voxels within a set of 300 spherical regions of interest (ROIs) in cortical, subcortical, and cerebellar areas (Seitzman et al., 2020). Each ROI has previously been assigned to one of 16 putative networks, including: somatomotor (SM), lateral somatomotor (SML), cingulo-opercular (CO), auditory (AUD), default mode (DMN), parietal memory (PMN), visual (VIS), fronto-parietal (FPN), salience (SAL), ventral attention (VAN), dorsal attention (DAN), medial temporal lobe (MTL), reward (REW), basal ganglia (BG), thalamus (THAL), cerebellum (CER) networks, as well as unassigned (NA) ROIs (Seitzman et al., 2020). For each scan, we calculated the 300 x 300 FC matrix as the Fisher-transformed Pearson correlation matrix of the final averaged BOLD timeseries between all ROIs. We then used the vectorized upper triangle of each correlation matrix (excluding auto-correlations; 44,850 total correlations) as the input features for predicting age. Since site and/or scanner differences between samples might confound neuroimaging estimates, we harmonized FC correlation matrices across sites and scanners using an empirical Bayes modeling approach (ComBat, see Supplementary Fig. S2) (Fortin et al., 2017; Johnson et al., 2007), which has recently been applied to FC data (Yu et al., 2018). We also performed analyses without ComBat and observed consistent results (see Supplementary Table S1, as well as Supplementary Figs S4 and S5).

2.7. Gaussian process regression (GPR)

Machine learning analyses were conducted using the Regression Learner application in Matlab 2021a (MathWorks, 2021a). Following previous models of brain-predicted age using structural imaging (Cole et al., 2015), we trained a Gaussian process regression (GPR, *fitrgp*() function) (MathWorks, 2021b; Rasmussen, 2003) model with a rational quadratic kernel function to predict chronological age using the harmonized, vectorized FC matrices as feature inputs in the training set. The σ hyperparameter was tuned by searching a range of values from 10^{-4} to $10^{*}SD_{age}$ using Bayesian optimization across 100 training evaluations. The optimal range of σ was found from ~10^{-4} to 1 (see Supplementary Fig. S3), and σ was set to .0385 for all subsequent models. All other hyperparameters were set to default values (basis function = constant, standardize = true, MathWorks, 2021b).

Model performance in the training set was assessed using 10-fold cross validation via the total proportion of variance explained (R^2), root-mean-squared error (*RMSE*), and mean absolute error (*MAE*) between true chronological age and the cross-validated age predictions merged across the 10 folds. We then evaluated generalizability of the trained GPR model to predict age in unseen data by applying the trained model to the held-out test set of healthy controls. Finally, we applied the same trained GPR model to separate analysis sets of symptomatic AD, preclinical AD, and amyloid-negative controls in order to derive estimates of FC-predicted brain age and test our hypotheses regarding AD-related group differences.

For each participant in the analysis sets, we calculated the FC-predicted brain age gap (FC-BAG) as the difference between model-predicted and chronological age. In order to correct for regression dilution commonly observed in similar models (Le et al., 2018; Liang et al., 2019; Smith et al., 2019), we residualized FC-BAG by including chronological age as a covariate when testing for group differences (Cole et al., 2017; Le et al., 2018). However, to avoid inflating estimates of prediction accuracy (Butler et al., 2021), only *uncorrected* age prediction values were used for evaluating model performance in the training and test sets. Greater residual FC-BAG estimates can be interpreted to reflect cases in which the pattern of FC appears older than expected given the participant's true age, after correcting for the age-dependent bias on the model prediction. We hypothesized that this pattern of elevated FC-BAG should be observed in preclinical and symptomatic AD.

2.8. Feature selection analyses

To explore which FC networks drove age prediction in the GPR model, we identified the strongest predictors of age by performing forward sequential feature selection (Pudil et al., 1994) in the full training sample of cognitively normal, amyloid-negative controls. Specifically, we used the *sequentialfs()* function in MatLab (MathWorks, 2021c) to identify FC network features that improved cross-validated age prediction accuracy in the fully-trained and optimized GPR model. Compared to backward feature selection methods (e.g., recursive feature elimination; Guyon and Elisseeff, 2003; Kohavi and Sommerfield, 2000), forward sequential feature selection may perform better when the number of important features is small (Aha and Bankert, 1996). Given that the aim of this analysis was to reduce the number of important features to an interpretable amount, forward selection was chosen over backward selection. In order to further improve interpretability, minimize collinearity between the 44,850 regional FC pairs, and reduce computational time, we performed feature selection at the level of functional networks (17 x 17 matrix), rather than ROIs (300 x 300 matrix). However, this network-level approach necessarily loses information regarding regional specificity and assumes that network-level averages adequately summarize regions within the networks.

To compare these age-predictive FC features to those that are most predictive of AD, we also performed forward sequential feature selection with support vector machine (SVM; MathWorks, 2021d) models. These analyses identified features that improved cross-validated classification accuracy between amyloid-negative controls and either preclinical AD or symptomatic AD participants. SVM hyperparameters for kernel function, box constraint, and kernel scale were tuned separately for preclinical and symptomatic SVM models using a similar Bayesian optimization approach.

2.9. Design and statistical analysis

We tested our hypotheses regarding symptomatic and preclinical AD by performing cross-sectional analyses of existing data. All statistical analyses were conducted in R 4.0.2. (R Core Team, 2020). Group differences in the AD samples were tested with independent-samples *t* tests for continuous variables and χ^2 tests for categorical variables, using the cognitively normal amyloid-negative controls as a reference group. FC-BAG was the main dependent variable of interest. We tested symptomatic and preclinical AD group differences with linear regression models. To correct for age-related bias in FC-BAG estimates (e.g., Le et al. 2018), as well as demographic differences between samples, we controlled for age, sex, years of education, and race as covariates during statistical tests. *Post hoc* pairwise group comparisons were tested with independent-samples *t* tests. For all independent-samples *t* tests, we tested the assumptions that residual FC-BAG was normally distributed with equal variance between groups, respectively, with the Shapiro-Wilk test of normality and Levene's test for equality of variances. To distinguish between effects of *APOE* genotype vs. AD pathology, we performed analyses with and without controlling for *APOE* genotype. Effect sizes were computed as partial η^2 (η_p^2).

2.10. Data availability

The data and code used in this study are available by request through the Knight ADRC (https://knightadrc.wustl.edu/research/resourcerequest.htm).

3. Results

3.1. Sample & demographics

A total of 391 participants were included in the training sets (137 Ances lab controls, 120 DIAN controls, and 134 Knight ADRC controls). An additional 98 participants were included in the test sets (38 Ances lab controls, 26 DIAN controls, and 34 Knight ADRC controls). Finally, 483 independent participants from the Knight ADRC were included in the analysis sets (145 amyloid-negative controls, 151 preclinical AD, and 156 symptomatic AD). Full demographic characteristics are reported in Table 1. Preclinical AD participants were significantly older ($t = 6.42$, $p < .001$) and more likely to be *APOE* $\varepsilon4$ carriers ($\chi^2 = 35.39$, $p < .001$) than amyloid-negative controls. Further, symptomatic AD participants were significantly older ($t = 9.80$, $p < .001$), more likely male ($\chi^2 = 9.56$, $p = .002$), more likely to be *APOE* $\varepsilon4$ carriers ($\chi^2 = 55.25$, $p < .001$), and had marginally fewer years of education ($t = 2.01$, $p < .046$) and lower MMSE scores ($t = 12.55$, $p < .001$) than amyloid-negative controls.

3.2. FC successfully predicts brain age in training and test sets

The GPR model was able to accurately predict chronological age from the FC matrices in the full training set of healthy controls as assessed using 10-fold cross validation. As shown in Fig. 1A, FC-predicted brain age was strongly correlated with chronological age ($R^2 = .682$) with an *MAE* of 8.587 years (*RMSE* = 10.441). Further, accurate model performance was generalizable to the held-out test set, as shown in Fig. 1B ($R^2 = .727$, *MAE* = 8.195, *RMSE* = 10.317).

3.3. Elevated FC-BAG in symptomatic AD

Residual FC-BAG was normally distributed in all groups defined by cognitive status (Shapiro-Wilk statistics > 0.99, *ps* > 0.39). Variance in residual FC-BAG did not differ between groups (Levene's statistic = 0.07, $p = 0.80$).

A linear regression model tested the effect of symptomatic AD (defined as CDR > 0 vs. CDR = 0 within the complete analysis sets) on FC-BAG, controlling for true age and demographic covariates (see Table 2A). FC-BAG was 2.88 years older in symptomatic AD participants compared to controls ($\beta = 2.88$, $p < 0.001$, $\eta_p^2 = 0.04$, see Fig. 2A and B, Table 2A). Importantly, the effect of symptomatic AD remained significant in the full model controlling for all biomarkers and covariates ($\beta = 3.71$, $p < 0.001$, $\eta_p^2 = 0.03$, see Table 2E).

Pairwise independent-samples *t* tests revealed that residual FC-BAG was only marginally elevated in CDR > 0.5 participants relative to CDR = 0 ($t = 1.64$, $p = .109$, see Supplementary Fig. 6), but did not differ significantly between CDR = 0.5 and CDR > 0.5 ($t = 0.07$, $p = .945$).

3.4. Reduced FC-BAG in preclinical AD

Residual FC-BAG was normally distributed in all groups defined by AD biomarkers (Shapiro-Wilk statistics > 0.98, *ps* > 0.29). Variance in residual FC-BAG did not differ between groups (Levene's statistic = 0.26, $p = 0.77$).

Another regression model tested the effect of preclinical AD (defined as cognitively normal amyloid-positive vs. amyloid-negative) on FC-BAG, controlling for age and demographic covariates (see Table 2B). FC-BAG was 1.92 years younger in preclinical AD participants compared to controls ($\beta = -1.92$, $p = .018$, $\eta_p^2 = 0.02$, Table 2B).

To explore whether the effects of preclinical AD pathology on FC-BAG were associated with the stages of amyloidosis (A- vs. A+) and/or tau pathophysiology (T- vs. T+), we further split the preclinical and control samples by tau positivity and simultaneously tested these effects in an additional linear model (see Table 2C). FC-BAG was 2.15 years younger in T+ compared to T- participants ($\beta = -2.15$, $p = .034$, $\eta_p^2 = 0.02$, see Fig. 2C and D, Table 2C). Controlling for tau, there was no difference between A+ and A- participants ($\beta = 0.03$, $p = .976$). Follow-up pairwise independent-samples *t* tests revealed that residual FC-BAG was significantly lower in A+T+ participants compared to A-T- ($t = 3.35$, $p < .001$, see Fig. 2D). However, the effect of tau was not significant in the full model controlling for all biomarkers and covariates ($\beta = -1.39$,

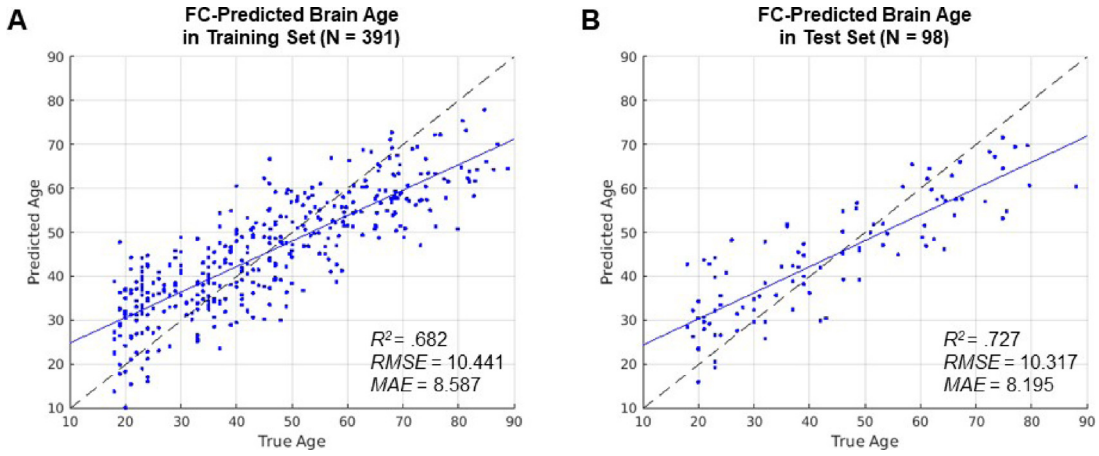

Fig. 1. Performance of the FC-predicted brain age model. Scatterplots show the cross-validated model predictions in the training set (A) and in the held-out test set (B). Age predicted by the model (y axis) is plotted against true age (x axis). Blue lines represent regression lines. Dashed black lines represent perfect prediction. Model performance is evaluated by proportion of variance explained (R^2), root-mean-square error (*RMSE*), and mean absolute error (*MAE*).

Table 2
Linear regression models predicting FC-BAG. Model estimates are presented as beta weight (standard error). CDR = Clinical Dementia Rating. *** $p < .001$, ** $p < .01$, * $p < .05$, ^ $p < .10$.

	MODELS				
	A. Symptomatic AD	B. Preclinical Amyloid	C. Preclinical Amyloid & Tau	D. Preclinical APOE	E. Full Model
Test Sample	All analysis sets	Cognitively normal only	Cognitively normal only	Cognitively normal only	All analysis sets
Predictors					
Intercept	32.39 (3.53)***	27.81 (4.24)***	33.22 (4.59)***	30.91 (4.28)***	33.54 (4.28)***
CDR > 0	2.88 (0.69)***				3.71 (1.17)**
Amyloid +		-1.92 (0.81)*	0.03 (0.99)		0.15 (0.99)
Tau +			-2.15 (1.01)*		-1.39 (0.92)
APOE ε4 +				-1.88 (0.78)*	-1.44 (0.80)^
Age (y)	-0.62 (0.04)***	-0.56 (0.05)***	-0.65 (0.05)***	-0.59 (0.05)***	-0.65 (0.05)***
Sex = female	-1.58 (0.63)*	-1.10 (0.79)	-1.25 (0.83)	-1.15 (0.79)	-1.44 (0.76)^
Education (y)	-0.07 (0.11)	-0.01 (0.15)	-0.01 (0.15)	-0.04 (0.15)	-0.001 (0.14)
Race = white	2.51 (0.93)**	2.18 (1.17)^	2.92 (1.53)^	2.11 (1.17)^	2.74 (1.47)^

$p = .135$, $\eta_p^2 = 0.01$, see Table 2E), and the effect of amyloid was not significant ($\beta = 0.15$, $p = .877$).

3.5. Reduced FC-BAG in APOE ε4 carriers

Residual FC-BAG was normally distributed in all groups defined by *APOE* genotype (Shapiro-Wilk statistics > 0.98, *ps* > 0.37). Variance in residual FC-BAG did not differ between groups (Levene's statistic = 0.37, $p = 0.55$).

A final regression model tested the effect of *APOE* genotype (defined as cognitively normal *APOE* ε4 carriers vs. *APOE* ε4 non-carriers) on FC-BAG, controlling for age and demographic covariates (see Table 2D). FC-BAG was 1.88 years younger in *APOE* ε4 carriers compared to non-carriers ($\beta = -1.88$, $p = .016$, $\eta_p^2 = 0.02$, see Fig. 2E and F, Table 2D). The effect of *APOE* was only marginally significant in the full model controlling for all biomarkers and covariates ($\beta = -1.44$, $p = .072$, $\eta_p^2 = 0.01$, see Table 2E).

3.6. Comparison of age and AD features

We used forward sequential feature selection to identify the FC networks that were the strongest predictors of age in a similar GPR model trained to predict age based on network-level FC (i.e., 153 intra- and inter-network FC summary measures). To validate this method, the network-level GPR model achieved moderate performance in predicting age ($R^2 = 0.52$). Further, SVM models using network-level FC discriminated between symptomatic AD and controls with 74% accuracy, although classification of preclinical AD was only modestly above chance (accuracy = 55%).

The forward sequential feature selection algorithm identified 32 FC features that most strongly predicted age. As shown in Fig. 3A, these features included a variety of intra-network (PMN x PMN, SAL x SAL, MTL x MTL, NA x NA) and inter-network connections (most prominently including inter-network connections with AUD and BG networks). Only 4 FC features were identified as strong predictors of preclinical AD (CER x CER, PMN x SML, FPN x AUD, and CER x PMN, see Fig. 3B). Finally, 10 FC features were identified as strong predictors of symptomatic AD (SM x SM, CO x CO, BG x BG, as well as inter-network connections prominently including the CO and DMN networks, see Fig. 3C).

As shown in Fig. 3D, only one feature was identified as an important predictor for both healthy age differences and preclinical AD (CER x PMN). However, there was no overlap in features that strongly predicted age and symptomatic AD, nor between preclinical and symptomatic AD.

4. Discussion

The present results offer several noteworthy findings. To review, our machine learning model successfully predicted chronological age from FC data. FC-based age predictions were significantly elevated in symptomatic AD compared to cognitively normal controls. Surprisingly, FC-based age predictions were also significantly *reduced* in preclinical AD compared to biomarker-negative controls, particularly in participants with positive amyloid and tau pathophysiology, and were also reduced in *APOE* ε4 carriers relative to non-carriers. Finally, FC features that were strongest predictors of healthy age differences mini-

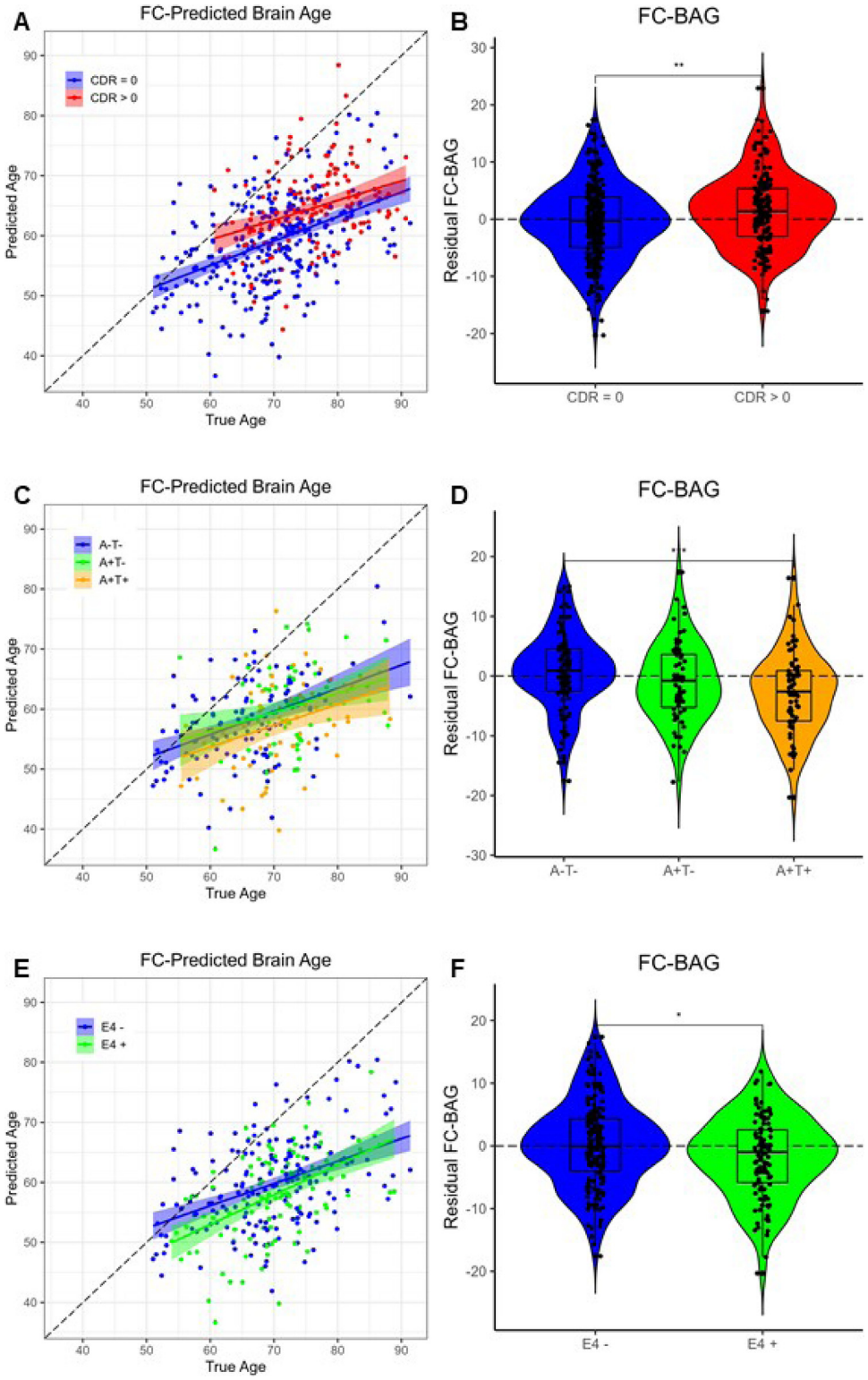

Fig. 2. Group differences in FC-predicted brain age in the analysis sets. Comparisons are presented between cognitively normal (CDR = 0, blue) vs. symptomatic AD (CDR > 0, red) (A, B); A-T- (blue) vs. A+T- (green) vs. A+T+ (gold) (C, D); and cognitively normal *APOE* ε4 carriers (blue) vs. non-carriers (green) (E, F). Scatterplots (A, C, E) show predicted vs. true age for each group. Colored lines and shaded areas represent group-specific regression lines and 95% confidence regions. Dashed black lines represent perfect prediction. Violin plots (B, D, F) show residual FC-BAG (controlling for true age) in each group. Group differences are reported from pairwise independent-samples *t* tests. *** $p < .001$, ** $p < .01$, * $p < .05$, $^{\wedge}$ $p < .10$.

mally overlapped with predictors of preclinical AD, and did not overlap with symptomatic AD. We now discuss each of these findings in turn.

4.1. Modeling brain age with FC

Our FC-based model successfully predicted chronological age in an adult lifespan sample with an *MAE* of about 8 years. Previous models, mostly trained on structural MRI data, have reported *MAE*s as low as 3 to 5 years (Bashyam et al., 2020; Cole and Franke, 2017; Fisch et al., 2021; Gong et al., 2021; Liem et al., 2017; Wang et al., 2019). Thus, the present model predicts age with lower accuracy compared to structural-based models, which is consistent with other direct comparisons between FC- and structural MRI-based age prediction models (Dunås et al., 2021; Eavani et al., 2018; Liem et al., 2017). The observed level of performance is more consistent with previous FC-predicted brain age models

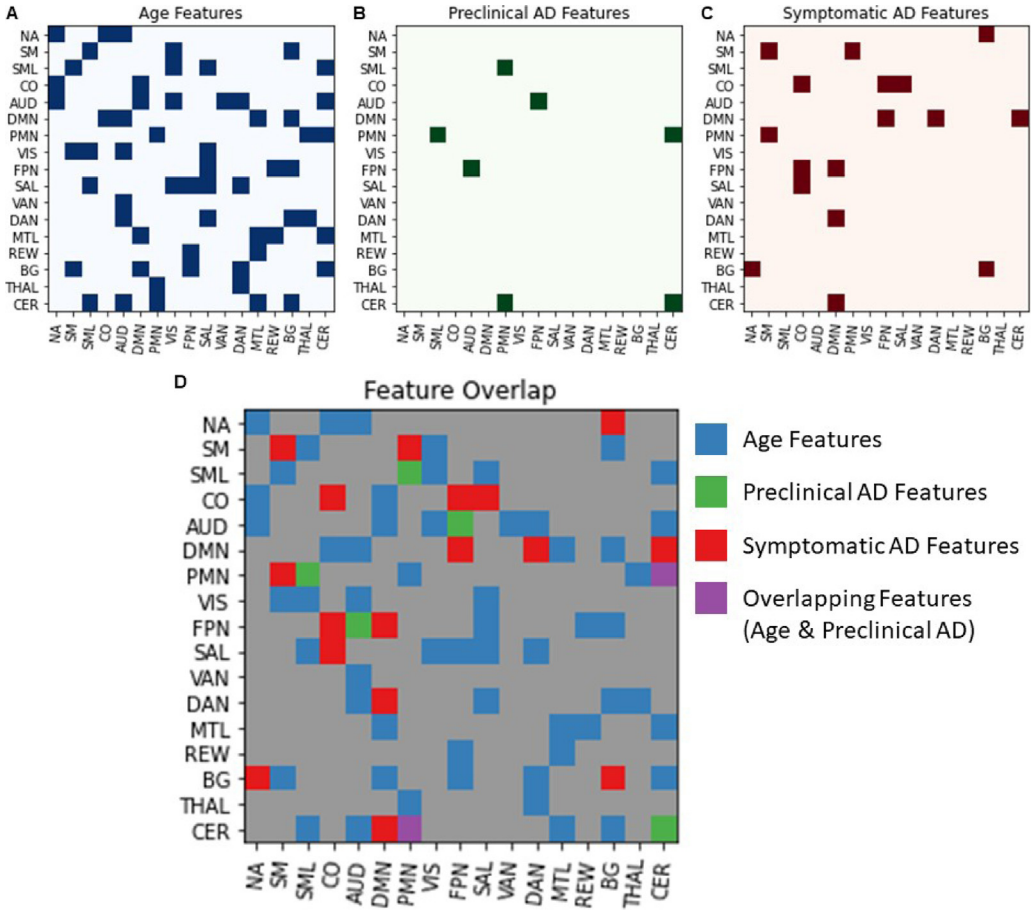

Fig. 3. Strongest FC predictors of (A) healthy age differences in the cognitively normal, amyloid-negative training set, (B) preclinical AD vs. amyloid-negative controls, and (C) symptomatic AD vs. amyloid-negative controls. Matrices display intra-network (on diagonal) and inter-network (off diagonal) FC features that were identified as strongest predictors via forward sequential feature selection (see methods). Overlapping features (D) are plotted for age, preclinical AD, and symptomatic AD.

in developmental (Dosenbach et al., 2010; Nielsen et al., 2019), older adult (Eavani et al., 2018), and adult lifespan samples (Dunås et al., 2021; Engemann et al., 2020; Gonneaud et al., 2021; Liem et al., 2017), which have achieved *MAE*s from 5 to 11 years. Moreover, although prediction accuracy is of course an essential part of evaluating brain age models, our application of this model is primarily motivated by the sensitivity of deviations in age prediction to disease status. Notably, BAG estimates in models with "moderate" accuracy are more discriminative of disease states than those from overly "tight" or "loose" age prediction models (Bashyam et al., 2020). Thus, the relatively low accuracy of the current age prediction model does not preclude its application as a sensitive measure of AD.

Importantly, our approach utilized conservative pre-processing and quality assurance methods to minimize the influence of head motion in FC estimates (Ciric et al., 2017; Power et al., 2014). Thus, our model likely captures meaningful signal related to age with minimal confounding influence of head motion. One further advantage of our approach was that we trained the model using data from samples that were well characterized in AD biomarkers and clinical assessments of dementia. Since undetected AD pathology may inflate age differences in FC estimates (Brier et al., 2014b), we excluded preclinical AD participants from the training sets to the greatest extent possible (Ly et al., 2020). Hence, the patterns of FC differences across the adult lifespan captured in our model most likely reflect the influence of healthy age differences with minimal confounding influence of AD pathology.

4.2. FC-predicted brain age as a marker of symptomatic AD

As predicted, our model estimates of FC-BAG were significantly elevated in symptomatic AD participants compared to cognitively normal controls. The mean difference in FC-BAG (about 3 years) was relatively small compared to previously reported effects in AD and MCI samples using structural-based brain age models (about 5 to 10 years) (Cole and Franke, 2017; Franke and Gaser, 2019). However, we note that the largest of these effects were reported in CDR 1 samples (Franke and Gaser, 2012), at a more affected disease stage than the current sample, including primarily CDR 0.5 individuals. Thus, FC may capture meaningful, but relatively small, signal that is sensitive to the earliest symptomatic stages of AD. However, in the 37 participants with CDR > 0.5 in the current sample, FC-BAG was not significantly elevated in CDR > 0.5 relative to CDR 0.5, as would be expected by this interpretation.

Importantly, this FC-related signal may capture complex disruptions of connectivity within and between networks, as have been previously described in early AD (Brier et al., 2014a). This FC signal may thus be distinct from AD-related atrophy, captured for instance in structural MRI. Hence, multimodal models of age-related functional and structural features may maximize sensitivity to AD. Indeed, recent studies have demonstrated the unique benefits of multimodal brain-age models in improving the accuracy of age prediction (Liem et al., 2017) and capturing heterogeneous patterns of advanced brain aging (Eavani et al., 2018; Smith et al., 2020).

4.3. FC-predicted brain age as a marker of preclinical AD

Perhaps the most novel aspect of this study was the analysis of brain-predicted age in the context of preclinical late onset AD pathology, which to our knowledge, has not been evaluated in previous brain-predicted age reports using FC. Surprisingly, we found that FC-BAG was significantly *reduced* by about 2 years in preclinical AD, compared to cognitively normal amyloid-negative controls. Interestingly, there was also a significant effect in the same direction for *APOE* ε4 carriers compared to non-carriers, suggesting that even cognitively normal individuals at increased genetic risk of AD demonstrate relatively "younger" patterns of FC. These results were in the opposite direction of our prediction that preclinical disruption of FC networks should produce *elevated* estimates of brain age. We offer some potential interpretations of this surprising observation.

First, it is possible that the relative reduction in FC-BAG in preclinical AD and the relative elevation in symptomatic AD may reflect a biphasic response to AD progression. Similar biphasic responses have been proposed in models of functional task activation (Jagust and Mormino, 2011) and functional connectivity (Wales and Leung, 2021). Observations of hyper-activation and hyper-connectivity, along with the present "younger" appearing pattern of FC in preclinical AD, may reflect a compensatory response to early AD pathology, allowing these individuals to maintain normal cognition despite accumulating pathology (Cabeza et al., 2018). This interpretation predicts that lower FC-BAG should be associated with better cognition in the preclinical AD sample. Other models posit that amyloid-related hyper-excitability and tau-related hypo-excitability emerge in neuronal circuits via protein-specific disruption of neurotransmitters (Harris et al., 2020). However, previous studies have reported patterns of hyper-connectivity in participants with positive amyloid accumulation and low tau, while the later preclinical stage of elevated tau is associated with hypo-connectivity (Schultz et al., 2017; Sepulcre et al., 2017). In contrast, we observed that reduced FC-BAG was most prominent in the A+T+ participants. Thus, if the present results indeed reflect a biphasic response of FC to AD progression, it appears to be lagging behind previous observations.

Alternatively, it is possible that the significant reduction in FC-BAG may indeed reflect genuine dysfunction of the functional networks in response to preclinical AD pathology. However, this pattern may be inconsistent with "older" appearing patterns of FC, and thus a model trained to predict age might detect some pathological variance as appearing "younger." Consistent with this interpretation, we identified minimal overlap in feature importance for FC networks predictive of age and AD, as discussed below. Further, the relative effects of preclinical AD and *APOE* ε4 positivity both went in the same negative direction, suggesting that both AD biomarker pathology and genetic risk are associated with reduced FC-BAG in cognitively normal samples. However, the effects we observed in preclinical AD and *APOE* ε4 were only marginally significant in the full model, which included terms for all biomarker and genetic factors, which may be collinear. Further, these effects were relatively small, and thus may be driven by sample-specific noise, or the younger age prediction may be driven by statistical artifacts related to regression dilution (see also 4.5 Limitations). Hence, future studies should attempt to replicate these results in independent samples.

4.4. Predictive FC features of age and AD

Importantly, although one inter-network FC feature (PMN x CER) was identified as a strong predictor for both healthy age differences and preclinical AD, overall, age and AD were predicted by mostly non-overlapping networks. Thus, AD likely produces disruptions in FC networks that are distinct from those disrupted in healthy age differences, as opposed to an accelerated age-like pattern. Nevertheless, we found that the model trained on age differences was indeed sensitive to both preclinical and symptomatic AD, as well as genetic risk of AD. This result may reflect a unique benefit of the brain-predicted age approach in comprehensively summarizing complex neuroimaging indicators of "brain health" into a simple summary estimate.

4.5. Limitations

One limitation of this study is that the training set included MRI scans merged across independent datasets, spanning a range of collection sites, scanner models, and acquisition sequence parameters. These differences may introduce noise and/or confounding variance into the FC features. We have attempted to mitigate this problem by: (1) limiting the sample to only data from Siemens 3T scanners using similar protocols; (2) processing all MRI data through common pipelines and quality assessments; and (3) statistically harmonizing across different sites and scanners before combining the datasets.

Unsurprisingly, both preclinical and symptomatic AD groups were significantly older than the amyloid – controls. We have attempted to correct for this difference by including age as a covariate in our statistical models, as has been done in similar reports (e.g., Cole et al. 2017, Le et al. 2018). This approach limits interpretation of the group effect, as group variance and age variance are intermixed (Miller and Chapman, 2001). However, we note that differences in FC-BAG went in opposite directions for preclinical and symptomatic AD groups. Thus, age-related biases cannot fully account for the present results.

Additionally, we only conducted cross-sectional analyses of FC-BAG. Longitudinal analyses would be useful to address intra-individual reliability and trajectory of brain age estimates as AD pathology progresses over time, and should be investigated in future studies.

Further, although the DIAN and Knight ADRC samples were well characterized in assessments of dementia and AD biomarkers, these measures were not available in all samples. We minimized the chance of including participants with undiagnosed AD pathology by excluding participants over the age of 50 if these measures were unavailable. Future brain-predicted age models would benefit by using more richly characterized datasets to exclude potentially confounding age-related pathology.

Tau positivity was determined in this study based on a median split of CSF pTau 181. Future studies might improve upon this approach by using an *a priori* validated threshold of positivity and/or using tau PET.

Feature selection analyses were based on models that only achieved modest (74% for symptomatic AD) to poor (55% for preclinical AD) classification accuracy. Thus, the features identified as strong predictors (especially of preclinical AD) may be unstable.

Finally, although the Ances lab controls were relatively diverse, participants in other samples were mostly white and highly educated. Hence, this model may not be generalizable to broader samples. Future models would benefit by using more representative training samples.

5. Conclusions

Overall, the present study suggests that FC is sensitive to differences across the adult lifespan and can be used to successfully predict brain age, even after carefully controlling for head motion and preclinical AD. Consistent with structural-based models, FC-predicted brain age might be sensitive in detecting symptomatic AD. Further, our results suggest that FC-BAG might also be sensitive to preclinical AD, as well as AD genetic risk, although interpretation of the unexpected direction of this relationship requires further investigation. Although age and AD were predicted by mostly non-overlapping FC features, the present FC-predicted brain age model significantly detected deviations in both symptomatic and preclinical AD. Hence, FC may provide useful, distinct signal in developing models of comprehensive brain health to be

used as biomarkers of AD, along with other neurological and psychiatric disorders.

Appendix 1

**Dominantly Inherited Alzheimer Network consortium: Full Name and Credentials

Sarah Adams, MS; Ricardo Allegri, PhD; Aki Araki; Nicolas Barthelemy, PhD; Randall Bateman,MD; Jacob Bechara, BS; Tammie Benzinger, MD, PhD; Sarah Berman, MD, PhD; Courtney Bodge, PhD; Susan Brandon, BS; William (Bill) Brooks, MBBS,MPH; Jared Brosch, MD, PhD; Jill Buck, BSN; Virginia Buckles, PhD; Kathleen Carter, PhD; Lisa Cash, BFA; Charlie Chen, BA; Jasmeer Chhatwal, MD,PhD; Patricio Chrem Mendez, MD; Jasmin Chua, BS; Helena Chui, MD; Laura Courtney, BS; Carlos Cruchaga, PhD; Gregory S Day, MD; Chrismary DeLaCruz, BA; Darcy Denner, PhD; Anna Diffenbacher, MS; Aylin Dincer, BS; Tamara Donahue, MS; Jane Douglas, MPh; Duc Duong, BS; Noelia Egido, BS; Bianca Esposito, BS; Anne Fagan, PhD; Marty Farlow, MD; Becca Feldman, BS,BA; Colleen Fitzpatrick, MS; Shaney Flores, BS; Nick Fox, MD; Erin Franklin, MS; Nelly Joseph-Mathurin, PhD; Hisako Fujii, PhD; Samantha Gardener, PhD; Bernardino Ghetti, MD; Alison Goate, PhD; Sarah Goldberg, MS,LPC,NCC; Jill Goldman, MS,MPhil,CGC; Alyssa Gonzalez, BS; Brian Gordon, PhD; Susanne Gräber-Sultan, PhD; Neill Graff-Radford, MD; Morgan Graham, BA; Julia Gray, MS; Emily Gremminger, BA; Miguel Grilo, MD; Alex Groves, ; Christian Haass, PhD; Lisa Häsler, MSc; Jason Hassenstab, PhD; Cortaiga Hellm, BA; Elizabeth Herries, BA; Laura Hoechst-Swisher, MS; Anna Hofmann, MD; Anna Hofmann, ; David Holtzman, MD; Russ Hornbeck, MSCS, MPM; Yakushev Igor, MD; Ryoko Ihara, MD; Takeshi Ikeuchi, MD; Snezana Ikonomovic, MD; Kenji Ishii, MD; Clifford Jack, MD; Gina Jerome, MS; Erik Johnson, MD, PHD; Mathias Jucker, PhD; Celeste Karch, PhD; Stephan Käser, PHD; Kensaku Kasuga, MD; Sarah Keefe, BS; William Klunk, MD, PHD; Robert Koeppe, PHD; Deb Koudelis, MHS,RN; Elke Kuder-Buletta, RN; Christoph Laske, PhD; Allan Levey, MD, PHD; Johannes Levin, MD; Yan Li, PHD; Oscar Lopez MD, MD; Jacob Marsh, BA; Ralph Martins, PhD; Neal Scott Mason, PhD; Colin Masters, MD; Kwasi Mawuenyega, PhD; Austin McCullough, PhD Candidate; Eric McDade, DO; Arlene Mejia, MD; Estrella Morenas-Rodriguez, MD, PhD; John Morris, MD; James Mountz, MD; Cath Mummery, PhD;Neelesh Nadkarni, MD, PhD; Akemi Nagamatsu, RN; Katie Neimeyer, MS; Yoshiki Niimi, MD; James Noble, MD; Joanne Norton,MSN, RN, PMHCNS-BC ; Brigitte Nuscher, ; Ulricke Obermüller, ; Antoinette O'Connor, MRCPI; Riddhi Patira , MD; Richard Perrin, MD, PhD; Lingyan Ping, PhD; Oliver Preische, MD; Alan Renton, PhD; John Ringman, MD; Stephen Salloway, MD; Peter Schofield, PhD; Michio Senda, MD, PhD; Nicholas T Seyfried, D.Phil; Kristine Shady, BA, BS; Hiroyuki Shimada, MD, PhD; Wendy Sigurdson, RN; Jennifer Smith, PhD; Lori Smith, PA-C; Beth Snitz, PhD; Hamid Sohrabi, PhD; Sochenda Stephens, BS, CCRP; Kevin Taddei, BS ; Sarah Thompson, PA-C; Jonathan Vöglein, MD; Peter Wang, PhD; Qing Wang, PhD; Elise Weamer, MPH; Chengjie Xiong, PhD; Jinbin Xu, PhD; Xiong Xu, BS, MS

Declaration of Competing Interest

The authors declare no conflicts of interests. JC Morris is funded by NIH grants # P30 AG066444; P01AG003991; P01AG026276; U19 AG032438; and U19 AG024904. Neither Dr. Morris nor his family owns stock or has equity interest (outside of mutual funds or other externally directed accounts) in any pharmaceutical or biotechnology company. Dr. Salloway reports personal fees from EISAI, NOVARTIS, GENENTECH, ROCHE, GEMVAX, AVID, and LILLY. Dr. Bateman is on the scientific advisory board of C2N Diagnostics and reports research support from Abbvie, Avid Radiopharmaceuticals, Biogen, Centene, Eisai, Eli Lilly and Company, Genentech, Hoffman-LaRoche, Janssen, and United Neuroscience.

Credit authorship contribution statement

Peter R. Millar: Conceptualization, Methodology, Software, Formal analysis, Writing – original draft, Writing – review & editing, Visualization. **Patrick H. Luckett:** Conceptualization, Methodology, Software, Writing – review & editing. **Brian A. Gordon:** Resources, Writing – review & editing, Supervision, Project administration, Funding acquisition. **Tammie L.S. Benzinger:** Resources, Writing – review & editing, Supervision, Project administration, Funding acquisition. **Suzanne E. Schindler:** Resources, Writing – review & editing, Project administration, Funding acquisition. **Anne M. Fagan:** Resources, Writing – review & editing, Project administration, Funding acquisition. **Carlos Cruchaga:** Resources, Writing – review & editing, Project administration, Funding acquisition. **Randall J. Bateman:** Resources, Writing – review & editing, Project administration, Funding acquisition. **Ricardo Allegri:** Resources, Writing – review & editing, Project administration, Funding acquisition. **Mathias Jucker:** Resources, Writing – review & editing, Project administration, Funding acquisition. **Jae-Hong Lee:** Resources, Writing – review & editing, Project administration, Funding acquisition. **Hiroshi Mori:** Resources, Writing – review & editing, Project administration, Funding acquisition. **Stephen P Salloway:** Resources, Writing – review & editing, Project administration, Funding acquisition. **Igor Yakushev:** Resources, Writing – review & editing, Project administration, Funding acquisition. **John C. Morris:** Resources, Writing – review & editing, Project administration, Funding acquisition. **Beau M. Ances:** Conceptualization, Methodology, Resources, Writing – review & editing, Supervision, Project administration, Funding acquisition.

Acknowledgments

This research was funded by grants from the National Institutes of Health (P01-AG026276, P01-AG03991, P30 AG0 66444, 5-R01-AG052550-03, 5-R01-AG057680-03, 1-R01-AG067505-01, 1S10RR022984-01A1), with generous support from the Paula and Rodger O. Riney Fund and the Daniel J. Brennan MD Fund. Data collection and sharing for this project was supported by The Dominantly Inherited Alzheimer's Network (DIAN, U19AG032438) funded by the National Institute on Aging (NIA), the German Center for Neurodegenerative Diseases (DZNE), Institute for Neurological Research Fleni, Partial support by the Research and Development Grants for Dementia from Japan Agency for Medical Research and Development, AMED, and the Korea Health Technology R&D Project through the Korea Health Industry Development Institute (KHIDI).

We thank the participants for their dedication to this project, Haleem Azmy, Anna Boerwinkle, and Dimitre Tomov for technical and processing support, and Manu Goyal for helpful comments. This manuscript has been reviewed by DIAN Study investigators for scientific content and consistency of data interpretation with previous DIAN Study publications. We acknowledge the altruism of the participants and their families and contributions of the DIAN research and support staff at each of the participating sites for their contributions to this study. We thank the personnel of the Administration, Biomarker, Biostatistics, Clinical, Genetics, and Neuroimaging Cores of the Knight ADRC, as well as the Administration, Biomarker, Biostatistics, Clinical, Cognition, Genetics, and Imaging Cores of DIAN.

Supplementary materials

Supplementary material associated with this article can be found, in the online version, at doi:10.1016/j.neuroimage.2022.119228.

References

Aha, D.W., Bankert, R.L., Fisher, D., Lenz, H.J., 1996. A comparative evaluation of sequential feature selection algorithms. In: Learning from Data: Lecture Notes in Statistics, 112. Springer, New York, NY, pp. 199–206. doi:10.1007/978-1-4612-2404-4_19.

Bashyam, V.M., Erus, G., Doshi, J., Habes, M., Nasralah, I., Truelove-hill, M., Srinivasan, D., Mamourian, L., Pomponio, R., Fan, Y., Launer, L.J., Masters, C.L., Maruff, P., Zhuo, C., Johnson, S.C., Fripp, J., Koutsouleris, N., Satterthwaite, T.D., Wolf, D., Gur, R.E., Gur, R.C., Morris, J.C., Albert, M.S., Grabe, H.J., Resnick, S., Bryan, R.N., Wolk, D.A., Shou, H., Davatzikos, C.Consortium, I., Consoritum, P.A. disease, ADNI, CARDIA, 2020. MRI signatures of brain age and disease over the lifespan based on a deep brain network and 14 468 individuals worldwide. Brain 1–13. doi:10.1093/brain/awaa160.

Bateman, R.J., Xiong, C., Benzinger, T.L.S., Fagan, A.M., Goate, A.M., Fox, N.C., Marcus, D.S., Cairns, N.J., Xie, X., Blazey, T.M., Holtzman, D.M., Santacruz, A., Buckles, V., Oliver, A., Moulder, K., Aisen, P.S., Ghetti, B., Klunk, W.E., McDade, E.M., Martins, R.N., Masters, C.L., Mayeux, R., Ringman, J.M., Rossor, M.N., Schofield, P.R., Sperling, R.A., Salloway, S.P., Morris, J.C., 2012. Clinical and biomarker changes in dominantly inherited Alzheimer's disease. N. Engl. J. Med. 367, 795–804. doi:10.1056/NEJMoa1202753.

Brier, M.R., Thomas, J.B., Ances, B.M., 2014a. Network dysfunction in Alzheimer's disease: refining the disconnection hypothesis. Brain Connect. 4, 299–311. doi:10.1089/brain.2014.0236.

Brier, M.R., Thomas, J.B., Snyder, A.Z., Benzinger, T.L.S., Zhang, D., Raichle, M.E., Holtzman, D.M., Morris, J.C., Ances, B.M., 2012. Loss of intranetwork and internetwork resting state functional connections with Alzheimer's disease progression. J. Neurosci. 32, 8890–8899. doi:10.1523/JNEUROSCI.5698-11.2012.

Brier, M.R., Thomas, J.B., Snyder, A.Z., Wang, L., Fagan, A.M., Benzinger, T.L.S., Morris, J.C., Ances, B.M., 2014b. Unrecognized preclinical Alzheimer disease confounds rs-fcMRI studies of normal aging. Neurology 83, 1613–1619. doi:10.1212/WNL.0000000000000939.

Butler, E.R., Chen, A., Ramadan, R., Le, T.T., Ruparel, K., Moore, T.M., Satterthwaite, T.D., Zhang, F., Shou, H., Gur, R.C., Nichols, T.E., Shinohara, R.T., 2021. Pitfalls in brain age analyses. Hum. Brain Mapp. 1–10. doi:10.1002/hbm.25533.

Cabeza, R., Albert, M., Belleville, S., Craik, F.I.M., Duarte, A., Grady, C.L., Lindenberger, U., Nyberg, L.H., Park, D.C., Reuter-Lorenz, P.A., Rugg, M.D., Steffener, J., Natasha Rajah, M., 2018. Maintenance, reserve and compensation: the cognitive neuroscience of healthy ageing. Nat. Rev. Neurosci. doi:10.1038/s41583-018-0068-2.

Cherubini, A., Caligiuri, M.E., Peran, P., Sabatini, U., Cosentino, C., Amato, F., 2016. Importance of Multimodal MRI in characterizing brain tissue and its potential application for individual age prediction. IEEE J. Biomed. Health Inform. 20, 1232–1239. doi:10.1109/JBHI.2016.2559938.

Chhatwal, J.P., Schultz, A.P., Johnson, K.A., Benzinger, T.L.S., Jack, C.R., Ances, B.M., Sullivan Caroline, A., Salloway, S.P., Ringman, J.M., Koeppe Robert, A., Marcus Daniel, S., Thompson, P., Saykin Andrew, J., Correia, S., Schofield Peter, R., Rowe Christopher, C., Fox Nick, C., Brickman Adam, M., Mayeux, R., McDade, E.M., Bateman, R.J., Fagan, A.M., Goate, A.M., Xiong, C., Buckles Virginia, D., Morris, J.C., Sperling, R.A., 2013. Impaired default network functional connectivity in autosomal dominant Alzheimer disease. Neurology 81, 736–744.

Ciric, R., Wolf, D.H., Power, J.D., Roalf, D.R., Baum, G.L., Ruparel, K., Shinohara, R.T., Elliott, M.A., Eickhoff, S.B., Davatzikos, C., Gur, R.C., Gur, R.E., Bassett, D.S., Satterthwaite, T.D., 2017. Benchmarking of participant-level confound regression strategies for the control of motion artifact in studies of functional connectivity. Neuroimage 154, 174–187. doi:10.1016/j.neuroimage.2017.03.020.

Clark, C.M., Schneider, J.A., Bedell, B.J., Beach, T.G., Bilker, W.B., Mintun, M.A., Pontecorvo, M.J., Hefti, F., Carpenter, A.P., Flitter, M.L., Krautkramer, M.J., Kung, H.F., Coleman, R.E., Doraiswamy, P.M., Fleisher, A.S., Sabbagh, M.N., Sadowsky, C.H., Reiman, E.M., Zehntner, S.P., Skovronsky, D.M., 2011. Use of florbetapir-PET for imaging β-amyloid pathology. JAMA 305, 275–283. doi:10.1001/jama.2010.2008.

Cole, J.H., Annus, T., Wilson, L.R., Remtulla, R., Hong, Y.T., Fryer, T.D., Acosta-Cabronero, J., Cardenas-Blanco, A., Smith, R., Menon, D.K., Zaman, S.H., Nestor, P.J., Holland, A.J., 2017. Brain-predicted age in down syndrome is associated with beta amyloid deposition and cognitive decline. Neurobiol. Aging 56, 41–49. doi:10.1016/j.neurobiolaging.2017.04.006.

Cole, J.H., Franke, K., 2017. Predicting age using neuroimaging: innovative brain ageing biomarkers. Trends Neurosci. 40, 681–690. doi:10.1016/j.tins.2017.10.001.

Cole, J.H., Leech, R., Sharp, D.J., 2015. Prediction of brain age suggests accelerated atrophy after traumatic brain injury. Ann. Neurol. 77, 571–581. doi:10.1002/ana.24367.

Cruchaga, C., Kauwe, J.S.K., Harari, O., Jin, S.C., Cai, Y., Karch, C.M., Benitez, B.A., Jeng, A.T., Skorupa, T., Carrell, D., Bertelsen, S., Bailey, M., McKean, D., Shulman, J.M., De Jager, P.L., Chibnik, L., Bennett, D.A., Arnold, S.E., Harold, D., Sims, R., Gerrish, A., Williams, J., Van Deerlin, V.M., Lee, V.M.Y., Shaw, L.M., Trojanowski, J.Q., Haines, J.L., Mayeux, R., Pericak-Vance, M.A., Farrer, L.A., Schellenberg, G.D., Peskind, E.R., Galasko, D., Fagan, A.M., Holtzman, D.M., Morris, J.C., Goate, A.M., 2013. GWAS of cerebrospinal fluid tau levels identifies risk variants for alzheimer's disease. Neuron 78, 256–268. doi:10.1016/j.neuron.2013.02.026.

Dennis, E.L., Thompson, P.M., 2014. Functional brain connectivity using fMRI in aging and Alzheimer's disease. Neuropsychol. Rev. 24, 49–62. doi:10.1007/s11065-014-9249-6.

Dosenbach, N.U.F., Nardos, B., Cohen, A.L., Fair, D.A., Power, J.D., Church, J.a, Nelson, S.M., Wig, G.S., Vogel, A.C., Lessov-schlaggar, C.N., Barnes, K.A., Dubis, J.W., Feczko, E., Coalson, R.S., Jr, J.R.P., Barch, D.M., Petersen, S.E., Schlaggar, B.L., 2010. Prediction of individual brain maturity using fMRI. Science 329, 1358–1361. doi:10.1126/science.1194144.Prediction.

Dunås, T., Wåhlin, A., Nyberg, L., Boraxbekk, C., 2021. Multimodal image analysis of apparent brain age identifies physical fitness as predictor of brain maintenance. Cereb. Cortex 1–15. doi:10.1093/cercor/bhab019.

Eavani, H., Habes, M., Satterthwaite, T.D., An, Y., Hsieh, M.K., Honnorat, N., Erus, G., Doshi, J., Ferrucci, L., Beason-Held, L.L., Resnick, S.M., Davatzikos, C., 2018. Heterogeneity of structural and functional imaging patterns of advanced brain aging revealed via machine learning methods. Neurobiol. Aging 71, 41–50. doi:10.1016/j.neurobiolaging.2018.06.013.

Engemann, D.A., Kozynets, O., Sabbagh, D., Lemaitre, G., Varoquaux, G., Liem, F., Gramfort, A., 2020. Combining magnetoencephalography with magnetic resonance imaging enhances learning of surrogate-biomarkers. elife 9, 1–33. doi:10.7554/eLife.54055.

Fagan, A.M., Mintun, M.A., Mach, R.H., Lee, S.Y., Dence, C.S., Shah, A.R., LaRossa, G.N., Spinner, M.L., Klunk, W.E., Mathis, C.A., DeKosky, S.T., Morris, J.C., Holtzman, D.M., 2006. Inverse relation between *in vivo* amyloid imaging load and cerebrospinal fluid Abeta;42 in humans. Ann. Neurol. 59, 512–519. doi:10.1002/ana.20730.

Fisch, L., Leenings, R., Winter, N.R., Dannlowski, U., Gaser, C., Cole, J.H., Hahn, T., 2021. Editorial: predicting chronological age from structural neuroimaging: the predictive analytics competition 2019. Front. Psychiatry 12, 2019–2021. doi:10.3389/fpsyt.2021.710932.

Fischl, B., 2012. FreeSurfer. Neuroimage2 62, 774–781. doi:10.1016/j.neuroimage.2012.01.021.FreeSurfer.

Fortin, J.P., Parker, D., Tunç, B., Watanabe, T., Elliott, M.A., Ruparel, K., Roalf, D.R., Satterthwaite, T.D., Gur, R.C., Gur, R.E., Schultz, R.T., Verma, R., Shinohara, R.T., 2017. Harmonization of multi-site diffusion tensor imaging data. Neuroimage 161, 149–170. doi:10.1016/j.neuroimage.2017.08.047.

Fox, M.D., Zhang, D., Snyder, A.Z., Raichle, M.E., 2009. The global signal and observed anticorrelated resting state brain networks. J. Neurophysiol. 101, 3270–3283. doi:10.1152/jn.90777.2008.

Franke, K., Gaser, C., 2019. Ten years of brainage as a neuroimaging biomarker of brain aging: what insights have we gained? Front. Neurol. 10. doi:10.3389/fneur.2019.00789.

Franke, K., Gaser, C., 2012. Longitudinal changes in individual *BrainAGE* in healthy aging, mild cognitive impairment, and alzheimer's disease. GeroPsych 25 (4), 235–245. doi:10.1024/1662-9647/a000074.

Franke, K., Ziegler, G., Klöppel, S., Gaser, C., 2010. Estimating the age of healthy subjects from T1-weighted MRI scans using kernel methods: exploring the influence of various parameters. Neuroimage 50, 883–892. doi:10.1016/j.neuroimage.2010.01.005.

Frisoni, G.B., Fox, N.C., Jack, C.R., Scheltens, P., Thompson, P.M., 2010. The clinical use of structural MRI in Alzheimer disease. Nat. Rev. Neurol. 6, 67–77. doi:10.1038/nrneurol.2009.215.

Gaser, C., Franke, K., Klöppel, S., Koutsouleris, N., Sauer, H., 2013. BrainAGE in mild cognitive impaired patients: predicting the conversion to Alzheimer's disease. PLoS One 8. doi:10.1371/journal.pone.0067346.

Gong, W., Beckmann, C.F., Vedaldi, A., Smith, S.M., Peng, H., 2021. Optimising a simple fully convolutional network for accurate brain age prediction in the PAC 2019 Challenge. Front. Psychiatry 12, 1–8. doi:10.3389/fpsyt.2021.627996.

Gonneaud, J., Baria, A.T., Binette, A.P., Gordon, B.A., Chhatwal, J.P., Cruchaga, C., Jucker, M., Levin, J., Salloway, S.P., Farlow, M., Gauthier, S., Benzinger, T.L.S., Morris, J.C., Bateman, R.J., Breitner, J.C.S., 2021. Accelerated functional brain aging in pre-clinical familial Alzheimer's disease. Nat. Commun. 1–17. doi:10.1038/s41467-021-25492-9.

Goyal, M.S., Blazey, T.M., Su, Y., Couture, L.E., Durbin, T.J., Bateman, R.J., Benzinger, T.L.S., Morris, J.C., Raichle, M.E., Vlassenko, A.G., 2019. Persistent metabolic youth in the aging female brain. Proc. Natl. Acad. Sci. U. S. A. 116, 3251–3255. doi:10.1073/pnas.1815917116.

Greicius, M.D., Srivastava, G., Reiss, A.L., Menon, V., 2004. Default-mode network activity distinguishes Alzheimer's disease from healthy aging: evidence from functional MRI. Proc. Natl. Acad. Sci. U. S. A. 101, 4637–4642. doi:10.1073/pnas.0308627101.

Guyon, I., Elisseeff, A., 2003. An introduction to variable and feature selection. J. Mach. Learn. Res. 3, 1157–1182. doi:10.1016/j.aca.2011.07.027.

Harris, S.S., Wolf, F., De Strooper, B., Busche, M.A., 2020. Tipping the scales: peptide-dependent dysregulation of neural circuit dynamics in Alzheimer's disease. J. Clean. Prod. 107, 417–435. doi:10.1016/j.neuron.2020.06.005.

Hedden, T., Van Dijk, K.R.A., Becker, J.A., Mehta, A., Sperling, R.A., Johnson, K.A., Buckner, R.L., 2009. Disruption of functional connectivity in clinically normal older adults harboring amyloid burden. J. Neurosci. 29, 12686–12694. doi:10.1523/JNEUROSCI.3189-09.2009.

Jack, C.R., Bennett, D.A., Blennow, K., Carrillo, M.C., Feldman, H.H., Frisoni, G.B., Hampel, H., Jagust, W.J., Johnson, K.A., Knopman, D.S., Petersen, R.C., Scheltens, P., Sperling, R.A., Dubois, B., 2016. A new classification system for AD , independent of cognition A /T / N : an unbiased descriptive classification scheme for Alzheimer disease biomarkers. Neurology 0, 1–10.

Jack, C.R., Knopman, D.S., Jagust, W.J., Petersen, R.C., Weiner, M.W., Aisen, P.S., Shaw, L.M., Vemuri, P., Wiste, H.J., Weigand, S.D., Lesnick, T.G., Pankratz, V.S., Donohue, M.C., Trojanowski, J.Q., 2013. Tracking pathophysiological processes in Alzheimer's disease: an updated hypothetical model of dynamic biomarkers. Lancet Neurol 12, 207–216. doi:10.1016/S1474-4422(12)70291-0.

Jagust, W.J., Mormino, E.C., 2011. Lifespan brain activity, β-amyloid, and Alzheimer's disease. Trends Cogn. Sci. 15, 520–526. doi:10.1016/j.tics.2011.09.004.

Johnson, W.E., Li, C., Rabinovic, A., 2007. Adjusting batch effects in microarray expression data using empirical Bayes methods. Biostatistics 8, 118–127. doi:10.1093/biostatistics/kxj037.

Kohavi, R., Sommerfield, D. A., 2000. System and method for selection of important attributes (*U.S. Patent No. 6,026,399)*. U.S. Patent and Trademark Office, Washington, DC.

Le, T.T., Kuplicki, R.T., McKinney, B.A., Yeh, H.-W., Thompson, W.K., Paulus, M.P., 2018. A nonlinear simulation framework supports adjusting for age when analyzing BrainAGE. Front. Aging Neurosci. 10, 1–11. doi:10.3389/fnagi.2018.00317.

Liang, H., Zhang, F., Niu, X., 2019. Investigating systematic bias in brain age estimation with application to post-traumatic stress disorders. Hum. Brain Mapp. 40, 3143–3152. doi:10.1002/hbm.24588.

Liem, F., Varoquaux, G., Kynast, J., Beyer, F., Kharabian Masouleh, S., Huntenburg, J.M., Lampe, L., Rahim, M., Abraham, A., Craddock, R.C., Riedel-Heller, S., Luck, T., Loeffler, M., Schroeter, M.L., Witte, A.V., Villringer, A., Margulies, D.S., 2017. Predicting

brain-age from multimodal imaging data captures cognitive impairment. Neuroimage 148, 179–188. doi:10.1016/j.neuroimage.2016.11.005.

Löwe, L.C., Gaser, C., Franke, K., 2016. The effect of the APOE genotype on individual BrainAGE in normal aging, Mild cognitive impairment, and Alzheimer's Disease. PLoS One 11, 1–25. doi:10.1371/journal.pone.0157514.

Ly, M., Yu, G.Z., Karim, H.T., Muppidi, N.R., Mizuno, A., Klunk, W.E., Aizenstein, H.J., 2020. Improving brain age prediction models: incorporation of amyloid status in Alzheimer's disease. Neurobiol. Aging 87, 44–48. doi:10.1016/j.neurobiolaging.2019.11.005.

Mathworks, 2021. Regression Learner App (R2021a). Natick, MA: The MathWorks Inc. www.mathworks.com/help/stats/regression-learner-app.html.

Mathworks, 2021. fitrgp( ) (R2021a). Natick, MA: The Mathworks, Inc. www.mathworks.com/help/stats/fitrgp.html.

Mathworks, 2021. sequentialfs( ) (R2021a). Natick, MA: The MathWorks Inc. https://www.mathworks.com/help/stats/sequentialfs.html.

Mathworks, 2021. fitcsvm( ) (R2021a). Natick, MA: The Mathworks, Inc. www.mathworks.com/help/stats/fitcsvm.html.

McKay, N.S., Gordon, B.A., Hornbeck, R.C., Jack, C.R., Koeppe, R.A., Flores, S., Keefe, S.J., Hobbs, D.A., Joseph-mathurin, N., Wang, Q., Rahmani, F., Chen, C.D., McCullough, A., Koudelis, D., Chua, J., Ances, B.M., Millar, P.R., Nickels, M., Perrin, R.J., Allegri, R., Berman, S.B., Brooks, W.S., Cash, D.M., Chhatwal, J.P., Farlow, M.R., Fox, N.C., Fulham, M.J., Ghetti, B., Graff-radford, N., Ikeuchi, T., Day, G.S., Klunk, W.E., Levin, J., Lee, J., Martins, R.N., Masters, C.L., McConathy, J., Mori, H., Noble, J.M., Rowe, C.C., Salloway, S.P., Sanchez-Valle, R., Schofield, P.R., Shimada, H., Shoji, M., Su, Y., Suzuki, K., Voglein, J., Yakushev, I., Swisher, L., Cruchaga, C., Hassenstab, J.J., Karch, C.M., McDade, E.M., Xiong, C., Morris, J.C., Bateman, R.J., Benzinger, T.L., 2022. Neuroimaging within the dominantly inherited Alzheimer's network (DIAN): PET and MRI. bioRxiv doi:10.1101/2022.03.25.485799.

McKhann, G.M., Knopman, D.S., Chertkow, H., Hyman, B.T., Jack, C.R., Kawas, C.H., Klunk, W.E., Koroshetz, W.J., Manly, J.J., Mayeux, R., Mohs, R.C., Morris, J.C., Rossor, M.N., Scheltens, P., Carrillo, M.C., Thies, B., Weintraub, S., Phelps, C.H., 2011. The diagnosis of dementia due to Alzheimer's disease: recommendations from the National Institute on Aging-Alzheimer's association workgroups on diagnostic guidelines for Alzheimer's disease. Alzheimer's Dement. 7, 263–269. doi:10.1016/j.jalz.2011.03.005.

Millar, P.R., Petersen, S.E., Ances, B.M., Gordon, B.A., Benzinger, T.L.S., Morris, J.C., Balota, D.A., 2020. Evaluating the sensitivity of resting-state BOLD Variability to age and cognition after controlling for motion and cardiovascular influences: a network-based approach. Cereb. Cortex 30, 5686–5701. doi:10.1093/cercor/bhaa138.

Miller, G.A., Chapman, J.P., 2001. Misunderstanding analysis of covariance. J. Abnorm. Psychol. 110, 40–48. doi:10.1037/0021-843X.110.1.40.

Mintun, M.A., Larossa, G.N., Sheline, Y.I., Dence, C.S., Lee, S.Y., MacH, R.H., Klunk, W.E., Mathis, C.A., Dekosky, S.T., Morris, J.C., 2006. [11C]PIB in a nondemented population: potential antecedent marker of Alzheimer disease. Neurology 67, 446–452. doi:10.1212/01.wnl.0000228230.26044.a4.

Morris, J.C., 1993. The clinical dementia rating (CDR): current version and scoring rules. Neurology 43, 2412–2414.

Nielsen, A.N., Greene, D.J., Gratton, C., Dosenbach, N.U.F., Petersen, S.E., Schlaggar, B.L., 2019. Evaluating the prediction of brain maturity from functional connectivity after motion artifact denoising. Cereb. Cortex 29, 2455–2469. doi:10.1093/cercor/bhy117.

Ortega, M., Brier, M.R., Ances, B.M., 2015. Effects of HIV and combination antiretroviral therapy on cortico-striatal functional connectivity. AIDS 29, 703–712. doi:10.1097/QAD.0000000000000611.

Power, J.D., Barnes, K.A., Snyder, A.Z., Schlaggar, B.L., Petersen, S.E., 2012. Spurious but systematic correlations in functional connectivity MRI networks arise from subject motion. Neuroimage 59, 2142–2154. doi:10.1016/j.neuroimage.2011.10.018.

Power, J.D., Mitra, A., Laumann, T.O., Snyder, A.Z., Schlaggar, B.L., Petersen, S.E., 2014. Methods to detect, characterize, and remove motion artifact in resting state fMRI. Neuroimage 84, 320–341. doi:10.1016/j.neuroimage.2013.08.048.

Pudil, P., Novovičová, J., Kittler, J., 1994. Floating search methods in feature selection. Pattern Recognit. Lett. 15, 1119–1125. doi:10.1016/0167-8655(94)90127-9.

R Core Team, 2020. R: A language and environment for statistical computing. R Foundation for Statistical Computing, Vienna, Austria.

Rasmussen, C.E., 2003. Advanced lectures on machine learning. In: Carbonell, J.G., Siekmann, J. (Eds.), Advanced Lectures on Machine Learning. Springer-Verlag, Berlin, pp. 63–71.

Schindler, S.E., Gray, J.D., Gordon, B.A., Xiong, C., Batrla-Utermann, R., Quan, M., Wahl, S., Benzinger, T.L.S., Holtzman, D.M., Morris, J.C., Fagan, A.M., 2018. Cerebrospinal fluid biomarkers measured by Elecsys assays compared to amyloid imaging. Alzheimer's Dement. 14, 1460–1469. doi:10.1016/j.jalz.2018.01.013.

Schultz, A.P., Chhatwal, J.P., Hedden, T., Mormino, E.C., Hanseeuw, B.J., Sepulcre, J., Huijbers, W., LaPoint, M., Buckley, R.F., Johnson, K.A., Sperling, R.A., 2017. Phases of hyperconnectivity and hypoconnectivity in the default mode and salience networks track with amyloid and Tau in clinically normal individuals. J. Neurosci. 37, 4323–4331. doi:10.1523/jneurosci.3263-16.2017.

Seitzman, B.A., Gratton, C., Marek, S., Raut, R.V, Dosenbach, N.U.F., Schlaggar, B.L., Petersen, S.E., Greene, D.J., 2020. A set of functionally-defined brain regions with improved representation of the subcortex and cerebellum. Neuroimage 206, 1–17. doi:10.1016/j.neuroimage.2019.116290.

Sepulcre, J., Sabuncu, M.R., Li, Q., El Fakhri, G., Sperling, R.A., Johnson, K.A., 2017. Tau and amyloid β proteins distinctively associate to functional network changes in the aging brain. Alzheimer's Dement. 13, 1261–1269. doi:10.1016/j.jalz.2017.02.011.

Shulman, G.L., Pope, D.L.W., Astafiev, S.V., McAvoy, M.P., Snyder, A.Z., Corbetta, M., 2010. Right hemisphere dominance during spatial selective attention and target detection occurs outside the dorsal frontoparietal network. J. Neurosci. 30, 3640–3651. doi:10.1523/JNEUROSCI.4085-09.2010.

Smith, R.X., Strain, J.F., Tanenbaum, A., Fagan, A., Hassenstab, J.J., McDade, E.M., Schindler, S.E., Gordon, B.A., Xiong, C., Chhatwal, J.P., Jack, C.R., Karch, C., Berman, S.B., Brosch, J., Lah, J., Brickman, A., Cash, D., Fox, N., Graff-Radford, N., Levin, J., Noble, J., Holtzman, D., Masters, C., Farlow, M.R., Laske, C., Schofield, P., Marcus, D., Morris, J.C., Benzinger, T., Bateman, R.J., Ances, B., 2021. Resting-state functional connectivity disruption as a pathological biomarker in autosomal dominant Alzheimer disease. Brain Connect. 1–33. doi:10.1089/brain.2020.0808.

Smith, S.M., Elliott, L.T., Alfaro-Almagro, F., McCarthy, P., Nichols, T.E., Douaud, G., Miller, K.L., 2020. Brain aging comprises many modes of structural and functional change with distinct genetic and biophysical associations. elife 9, 1–28. doi:10.7554/eLife.52677.

Smith, S.M., Vidaurre, D., Alfaro-Almagro, F., Nichols, T.E., Miller, K.L., 2019. Estimation of brain age delta from brain imaging. Neuroimage 200, 528–539. doi:10.1016/j.neuroimage.2019.06.017.

Su, Y., D'Angelo, G.M., Vlassenko, A.G., Zhou, G., Snyder, A.Z., Marcus, D.S., Blazey, T.M., Christensen, J.J., Vora, S., Morris, J.C., Mintun, M.A., Benzinger, T.L.S., 2013. Quantitative analysis of PiB-PET with FreeSurfer ROIs. PLoS One 8. doi:10.1371/journal.pone.0073377.

Su, Y., Flores, S., Wang, G., Hornbeck, R.C., Speidel, B., Joseph-Mathurin, N., Vlassenko, A.G., Gordon, B.A., Koeppe, R.A., Klunk, W.E., Jack, C.R., Farlow, M.R., Salloway, S.P., Snider, B.J., Berman, S.B., Roberson, E.D., Brosch, J., Jimenez-Velazques, I., van Dyck, C.H., Galasko, D., Yuan, S.H., Jayadev, S., Honig, L.S., Gauthier, S., Hsiung, G.Y.R., Masellis, M., Brooks, W.S., Fulham, M., Clarnette, R., Masters, C.L., Wallon, D., Hannequin, D., Dubois, B., Pariente, J., Sanchez-Valle, R., Mummery, C., Ringman, J.M., Bottlaender, M., Klein, G., Milosavljevic-Ristic, S., McDade, E.M., Xiong, C., Morris, J.C., Bateman, R.J., Benzinger, T.L.S., 2019. Comparison of Pittsburgh compound B and florbetapir in cross-sectional and longitudinal studies. Alzheimer's Dement. 11, 180–190. doi:10.1016/j.dadm.2018.12.008, Diagnosis, Assess. Dis. Monit..

Thomas, J.B., Brier, M.R., Snyder, A.Z., Vaida, F.F., Ances, B.M., 2013. Pathways to neurodegeneration: effects of HIV and aging on resting-state functional connectivity. Neurology 80, 1186–1193. doi:10.1212/WNL.0b013e318288792b.

Vlassenko, A.G., McCue, L., Jasielec, M.S., Su, Y., Gordon, B.A., Xiong, C., Holtzman, D.M., Benzinger, T.L.S., Morris, J.C., Fagan, A.M., 2016. Imaging and cerebrospinal fluid biomarkers in early preclinical alzheimer disease. Ann. Neurol. 80, 379–387. doi:10.1002/ana.24719.

Volluz, K.E., Schindler, S.E., Henson, R.L., Xiong, C., Gordon, B.A., Benzinger, T.L.S., Holtzman, D.M., Morris, J.C., Fagan, A.M., 2021. Correspondence of CSF biomarkers measured by Lumipulse assays with amyloid PET. Alzheimer's Dement 17, e51085. https://doi.org/10.1002/alz.051085.

Wales, R.M., Leung, H., 2021. MS: the effects of amyloid and tau on functional network connectivity in older populations. Brain Connect. doi:10.1089/brain.2020.0902.

Wang, J., Knol, M.J., Tiulpin, A., Dubost, F., De Bruijne, M., Vernooij, M.W., Adams, H.H.H., Ikram, M.A., Niessen, W.J., Roshchupkin, G.V., 2019. Gray matter age prediction as a biomarker for risk of dementia. Proc. Natl. Acad. Sci. U. S. A. 116, 21213–21218. doi:10.1073/pnas.1902376116.

Yu, M., Linn, K.A., Cook, P.A., Phillips, M.L., McInnis, M., Fava, M., Trivedi, M.H., Weissman, M.M., Shinohara, R.T., Sheline, Y.I., 2018. Statistical harmonization corrects site effects in functional connectivity measurements from multi-site fMRI data. Hum. Brain Mapp. 39, 4213–4227. doi:10.1002/hbm.24241.